

Proposal of Pancake Axial-Air-Gap-Type Self-Excited Wound-Field Synchronous Motor

Masahiro Aoyama, *IEEE member*

Department of Environment and Energy System,
Graduate School of Science and Technology,
Shizuoka University / SUZUKI Motor Corporation
3-5-1 Johoku, Naka-Ku, Hamamatsu,
Shizuoka 432-8561, Japan
aoyamam@hhq.suzuki.co.jp

Toshihiko Noguchi, *IEEE Senior Member*

Department of Electrical and Electronics Engineering,
Graduate School of Engineering,
Shizuoka University
3-5-1 Johoku, Naka-Ku, Hamamatsu,
Shizuoka 432-8561, Japan
tnogut@ipc.shizuoka.ac.jp

Abstract— This paper proposes a pancake type synchronous motor where the space harmonics power is effectively utilized for the field magnetization instead of the permanent magnets. The pancake axial-gap structure, i.e., a single stator with double rotor configuration, can take great advantage to improve the mutual inductance which is indispensable for self-excitation of the magnet field. The advantages of the proposed motor in terms of the torque density is clarified with the FEM based simulation results. In addition, preliminary experimental test result is demonstrated from the viewpoint of the principle of self-excitation.

Keywords—synchronous motor; self-excitation, wound-field, space harmonics, axial-gap, finite element method.

I. INTRODUCTION

Reduction of the fuel consumption and the global warming gas emission is strongly demanded from the view point of the environmental conservation, and the development of such technologies is urgent matter particularly in the automotive sector. Applying electric components to the automotive power train brings a greater impact than minor improvement of the conventional internal combustion engines because it is rather difficult to improve the efficiency in the low-load range with the engines. An electric machine is one of the key components in the hybrid vehicles (HEVs) and the electric vehicles (EVs) in terms of the dynamic drivability and the fuel consumption performance. In general, an IPM (Interior Permanent Magnet) motor is often applied to the HEVs owing to its highly improved efficiency and specific power capability per physical volume. Permanent magnets used in the IPM motor are extremely expensive because Nd-Fe-B magnets are commonly employed to realize the high power density and to improve the fuel efficiency in the low-load operation for a street use [1]. Moreover, the traction motors are usually installed on the chassis where special countermeasures must be taken for environmental issues. In order to mitigate demagnetization caused by the temperature rise of the permanent magnets for example, costly rare-earth metals such as Dy and Tb must be added to the Nd-Fe-B magnets. Therefore, varieties of the rare-earth-free motors, particularly wound-field synchronous motor which replaces the permanent magnets with the

electromagnets are focused on due to remarkable rise of the Nd-Fe-B magnet market price [2][3]. These separate-excited wound-field machines, i.e., the wound-field flux switching motor have an advantage of the robust rotor structure even in the high-speed operation. The great merit of the high-speed operation is the weight reduction of the machine. The torque density of these motors is, however, lower than that of the commonly designed IPMSM, because it cannot utilize the reluctance torque but only the electromagnet torque which is generated by the DC field excitation. Recently, the self-excited wound-field synchronous motor that utilizes the space harmonics for the field magnetization has been studied in the industries for the automotive traction applications [4]-[9]. This self-excitation technique with diode-rectifier can be found in the old paper [10]-[20]. The self-excitation technique can eliminate an additional auxiliary chopper circuit for the DC-coil on the primary side. In addition, it has potential to obtain a position of the post IPMSM by achieving the comparable torque density with a rare-earth free configuration. Because it can utilize both the reluctance torque and the self-excited electromagnet torque. In the past works [4]-[6], however, it cannot be effectively retrieved the space harmonics power. The authors proposed an alternative rare-earth-free motor utilizing the space harmonics for the field magnetization power [7]-[9]. The proposed motor is based on the same self-excitation principle, but, can efficiently retrieve the space harmonics power by placing auxiliary poles on the q -axis. Figure 1 shows a simplified salient pole model of the motor. As can be seen in the figure, the motor model which proposed in [7]-[9] can improve the stator-rotor coupling coefficient of the leakage magnetic flux by the effect of auxiliary poles, compared with the benchmark model reported in reference [4]-[6]. The electromagnet torque caused by the space harmonics power and the reluctance torque caused by the double saliency are simultaneously generated in the proposed motor, but the electromagnet torque generated by the auxiliary poles and the salient poles on the rotor takes significant part of the total torque. Because the induced voltage in the rotor windings of the self-excited wound-field motor is unexpectedly reduced in the low-speed range, the strong stator-rotor coupling coefficient of the leakage magnetic flux, which is the main factor of the electromagnet torque generation, is significantly

important. The leakage magnetic flux of stator back yoke side was unable to be utilized effectively for the field magnetization on the proposed motor [7]-[9].

In this paper, the drawbacks of the self-excited synchronous motor are solved, and a novel self-excitation mechanism is proposed, focusing on the back-yoke-less stator and double rotor axial air gap configuration as shown in Fig. 1(c).

II. PROPOSED AXIAL AIR GAP MOTOR

Figure 2 shows a mechanical configuration of the proposed pancake axial-air-gap-type self-excited wound-field synchronous motor where the single concentrated winding stator without stator back-yoke and the double salient pole rotor are employed, and the rotor coils are added to the rotor salient poles. The rotor has two sorts of windings, i.e., an induction coil (I-coil) that retrieves mainly the second space harmonics power and an excitation coil (E-coil) for the field magnetization. The I-coil is placed around the outer diameter part to retrieve the space harmonics power efficiently. The both coils are connected in pole-pair via a diode rectifying circuit as shown in Fig. 3. Every rotor and stator coil is preformed so as to make them flat angle alpha windings to improve the coil space factor. Specifications of the motor are listed in Table I. Because enough rotor coil magnetomotive force could be found by assuming a double sided rotor, the proposed motor performed design without auxiliary poles.

III. SELF-EXCITATION PRINCIPLE AND MATHEMATICAL ANALYSIS OF TORQUE GENERATION

A. Magnetomotive Force of Concentrated Winding

The magnetomotive force generated by the concentrated winding structure has the second-order space harmonic on the fundamental magnetic field. Figure 4(a) shows magnetic flux density waveforms in the air gap, where the distributed winding structure of 12 poles-72 slots (1-to-6-slot-combination) and the concentrated winding structure of 12 poles-18-slots (2-to-3-slot-combination) are compared. Figure 4(b) shows harmonic contents of the magnetic flux density, which is analyzed by Fourier series and a developed formula of Fourier series of Fig. 4(a). As can be seen in Fig. 4, the magnetic flux waveform of the distributed winding structure is basically sinusoidal, except for the slot harmonics. However, the waveform of the concentrated winding structure is distorted by the second-order harmonic component. The second-order harmonic component is caused because every phase winding is wound separately on an individual tooth without superposition on the other phase windings.

B. Mathematical Model on dq Reference Frame

The motor with the 2-to-3-slot-combination has a d -axis inductance composed with a constant part and a periodical third time harmonic part caused by the rotation. Therefore, the d -axis rotor self-inductance L_{rd} and the q -axis rotor self-inductance L_{rq} can be given by

$$L_{rd}(\omega t) = L_{rd0} + L_{rda} \cos 3\omega t, \quad (1)$$

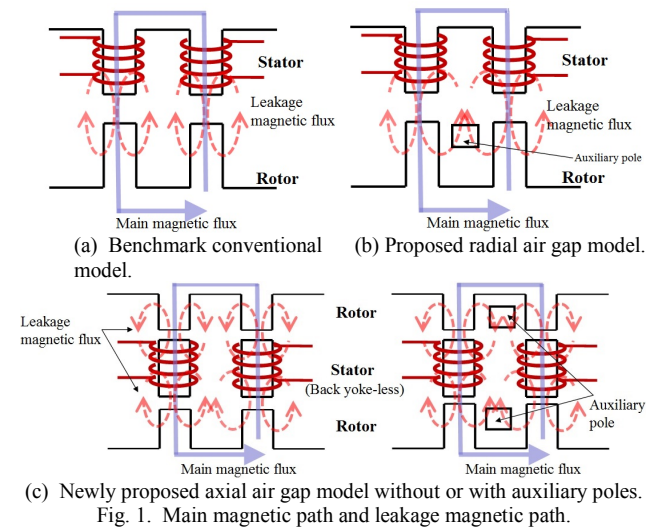


Fig. 1. Main magnetic path and leakage magnetic path.

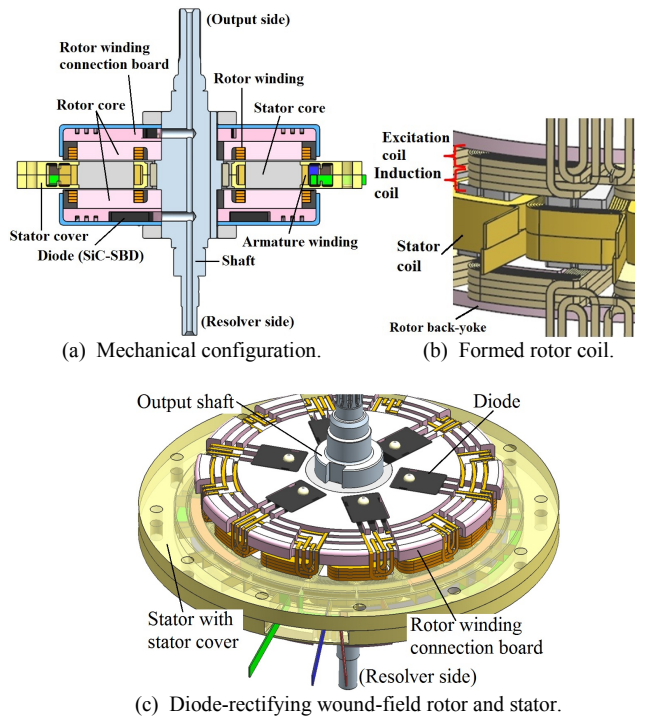


Fig. 2. Mechanical configuration of proposed axial air gap motor.

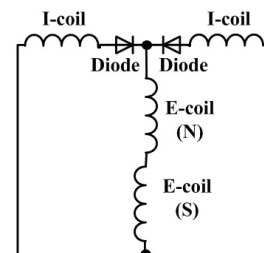


Fig. 3. Rotor winding connection using full-bridge rectifier.

$$L_{rq}(\omega t) = L_{rq0} + L_{rqa} \cos \left(3\omega t - \frac{\pi}{6} \right), \quad (2)$$

where L_{rd0} and L_{rq0} are the constant parts, and L_{rda} and L_{rqa} are the amplitudes of the periodical variations [9]. ω is an electrical synchronous angular velocity. The mathematical model of the proposed motor can be expressed as the following voltage equation:

$$\begin{aligned} \begin{bmatrix} v_{sd} \\ v_{sq} \\ v_{rd} \\ v_{rq} \end{bmatrix} &= \begin{bmatrix} R_s & 0 & 0 & 0 \\ 0 & R_s & 0 & 0 \\ 0 & 0 & R_r & 0 \\ 0 & 0 & 0 & R_r \end{bmatrix} \begin{bmatrix} i_{sd} \\ i_{sq} \\ i_{rd} \\ i_{rq} \end{bmatrix} + \begin{bmatrix} p & -\omega & p & -\omega \\ \omega & p & \omega & p \\ p & 0 & p & 0 \\ 0 & p & 0 & p \end{bmatrix} \begin{bmatrix} \psi_{sd} \\ \psi_{sq} \\ \psi_{rd} \\ \psi_{rq} \end{bmatrix} \\ &= \begin{bmatrix} R_s & 0 & 0 & 0 \\ 0 & R_s & 0 & 0 \\ 0 & 0 & R_r & 0 \\ 0 & 0 & 0 & R_r \end{bmatrix} \begin{bmatrix} i_{sd} \\ i_{sq} \\ i_{rd} \\ i_{rq} \end{bmatrix} + \begin{bmatrix} L_{sd} & 0 & M_d & 0 \\ 0 & L_{sq} & 0 & M_q \\ M_d & 0 & L_{rd} & 0 \\ 0 & M_q & 0 & L_{rq} \end{bmatrix} p \begin{bmatrix} i_{sd} \\ i_{sq} \\ i_{rd} \\ i_{rq} \end{bmatrix}, \\ &+ \begin{bmatrix} pL_{sd} & 0 & pM_d & 0 \\ 0 & pL_{sq} & 0 & pM_q \\ pM_d & 0 & pL_{rd} & 0 \\ 0 & pM_q & 0 & pL_{rq} \end{bmatrix} \begin{bmatrix} i_{sd} \\ i_{sq} \\ i_{rd} \\ i_{rq} \end{bmatrix} \\ &+ \omega \begin{bmatrix} 0 & -(L_{sq} + M_q) & 0 & -(M_q + L_{rq}) \\ L_{sd} + M_d & 0 & M_d + L_{rd} & 0 \\ 0 & 0 & 0 & 0 \\ 0 & 0 & 0 & 0 \end{bmatrix} \begin{bmatrix} i_{sd} \\ i_{sq} \\ i_{rd} \\ i_{rq} \end{bmatrix} \end{aligned} \quad (3)$$

where v_{sd} , v_{sq} , i_{sd} and i_{sq} are the armature voltages and currents, v_{rd} , v_{rq} , i_{rd} and i_{rq} are the d -axis and q -axis rotor winding voltages and currents, R_s and R_r are the armature winding and rotor winding resistances, M_d and M_q are the d -axis and q -axis mutual inductances, and p denotes a differential operator, respectively [9].

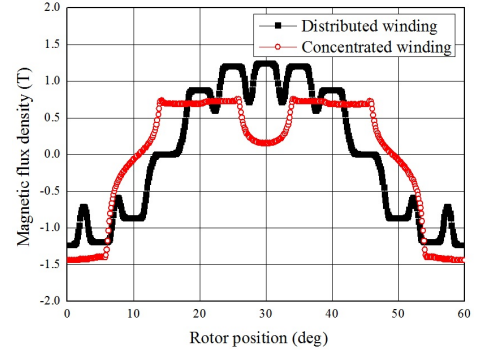
The output torque of the proposed motor is obtained by the vector product between the armature current and the magnetic flux, which is associated with the fourth term in Eq. (3):

$$\begin{aligned} T &= P_p \begin{bmatrix} i_{sd} & i_{sq} \end{bmatrix} \begin{bmatrix} 0 & -(L_{sq} + M_q) & 0 & -(M_q + L_{rq}) \\ L_{sd} + M_d & 0 & M_d + L_{rd} & 0 \end{bmatrix} \begin{bmatrix} i_{sd} \\ i_{sq} \\ i_{rd} \\ i_{rq} \end{bmatrix} \\ &= P_p (L_{sd} - L_{sq}) i_{sd} i_{sq} \\ &+ P_p \{ (M_d - M_q) i_{sd} i_{sq} - (M_q + L_{rq}) i_{sd} i_{rq} + (M_d + L_{rd}) i_{rd} i_{sq} \} \end{aligned} \quad (4)$$

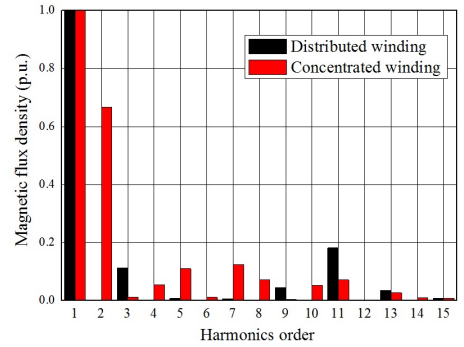
where P_p is the pole-pair number. As expressed in the above expression, the output torque is composed of the two terms, i.e., the reluctance torque and the electromagnet torque. Since the field current generating the electromagnet torque is proportional to ω , the benchmark model which is suggested in cannot deliver the sufficient torque in the low-speed range [7]-[9]. However, the newly proposed axial air gap motor can solve the problem by improving the stator-rotor coupling coefficient of the mutual inductance, which is the advantageous point brought by the stator-yoke-less double sided rotor structure.

TABLE I SPECIFICATIONS OF PROPOSED AXIAL AIR GAP MOTOR.

Number of poles	12
Number of slots	18
Stator outer diameter	120 mm
Axial length of core	34 mm
Air gap length	0.7 mm
Armature magnetomotive force	806.4 A _{rms} T
Number of I-pole coil-turn	21
Number of E-pole coil-turn	21
Core material	SMC (somaloy 3P)



(a) Magnetic flux density waveforms along air gap.



(c) Harmonic contents of magnetic flux density.

Fig. 4. Magnetic flux density along air gap under no-load.

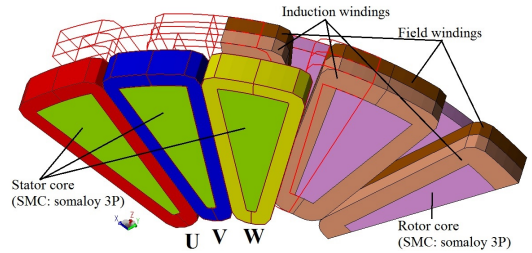


Fig. 5. Simulation model of proposed motor.

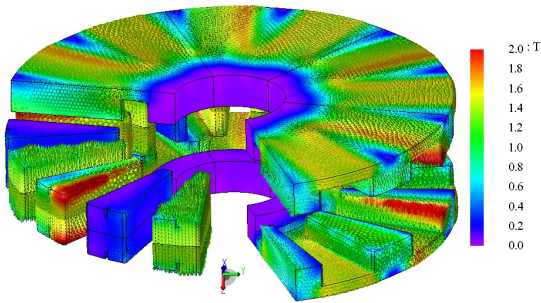


Fig. 6. Magnetic flux vector and magnetic flux density.

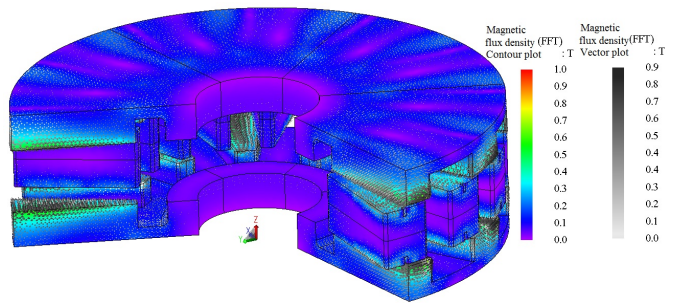


Fig. 7. Third time harmonic vector and magnetic flux density.

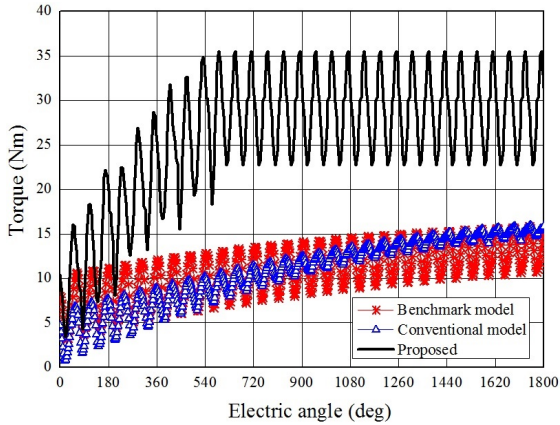


Fig. 8. Torque waveforms for 1000 r/min under MTPA control.

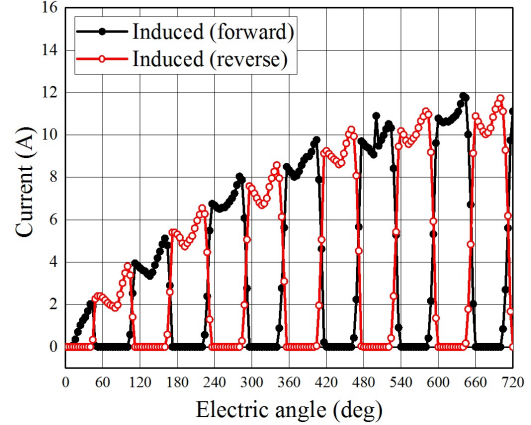
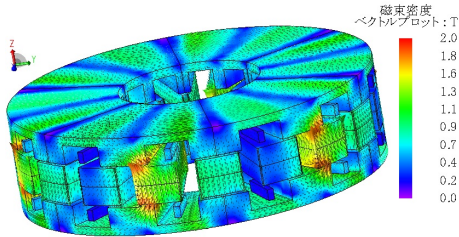
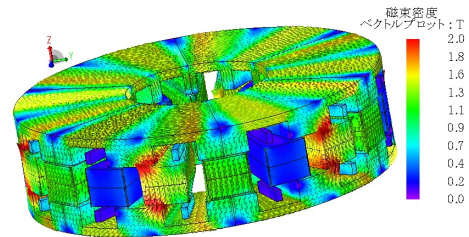


Fig. 9. Induced current waveforms of rotor coils for 1000 r/min under MTPA control.



(a) Before rotor magnetization. (in transient state).



(b) After rotor magnetization. (in steady state).

Fig. 10. Magnetic flux density and vector.

IV. ELECTROMAGNETIC FIELD ANALYSIS

The torque characteristics are calculated by using a divided three-dimensional model as shown in Fig. 5. Figure 6 shows the magnetic flux vector and flux density under the condition of the maximum armature magnetomotive force with MTPA control calculated by the magnetic field analysis. As shown in this figure, it can be confirmed that the electromagnetic force of circumferential direction, i.e., torque, occurs in double sided rotor. Figure 7 shows the second space harmonics vector, the magnetic density and the flux lines of the proposed model. It is found that the second space harmonic flux (the third time harmonic on rotating reference frame) utilized for the field magnetization links deeply into the double rotor in the proposed motor. Figure 8 shows the torque characteristics for 1000 r/min under the condition of the maximum armature magnetomotive force with MTPA control calculated by the magnetic field analysis. As shown in the figure, pancake axial-

air-gap-type self-excited wound-field structure greatly contributes to increase the average output torque. Figure 9 shows the rotor current waveforms (induced current) in the condition of Fig. 8. By referring to rotor current waveforms in Fig. 9, the induced current flows forward and reverse at time intervals. Thus, it can be easily confirmed that the third time harmonic on rotating reference frame (the second space harmonic on static coordinates) links to rotor windings and the electromagnet poles can be obtained by field current generated with full bridge rectifier as shown in Fig. 3. Figure 10 shows a process of the rotor magnetization, which is generated by self-excitation, in the transient state. Low torque ripple is observed in the region where the rotor magnetization, which is depend on electrical time constant, is completely formed.

V. PROTOTYPE MACHINE

Figure 11 shows the prototype machine with a proposed self-excited wound-field rotor, a back-yoke-less concentrated

stator with stator cover, a single stator and double sided rotor and motor assy. The wound-field rotor is mechanically reinforced by a resin mold to prevent destruction by the centrifugal force caused by a high speed rotation and to ensure electric insulation.

VI. PRELIMINARY EXPERIMENTAL TEST RESULTS

The rotor induced current in the diode forward direction for one pole pair is measured with a slip ring to demonstrate the self-excitation by the third time harmonic on rotating reference frame (the second space harmonic on static coordinates). Figure 11 shows the stator armature current (U-phase) and rotor current waveforms for 500 r/min under 40 A_{rms} of the stator armature current. The inverter carrier frequency is set at 10 kHz. In the preliminary experimental test, the load test of the motor is limited in the low speed range and low load condition. It is because the balanced of rotor assembly with slip ring did not mechanically proved, beside the machine parts are manually assembled. By referring to rotor current waveform in Fig. 11, it can be confirmed that the rotor current have a periodical 3ω component according to rotation. Thus, it can be easily confirmed that the third time harmonic on the rotating reference frame (the second space harmonic on static coordinates) links to rotor windings. The preliminary torque characteristics with respect to current phase under armature current 40 A_{rms} which is shown in Fig. 12, of proposed pancake axial-air-gap type rare-earth-free motor is investigated by controlling speed at a bench, and controlling torque with inverter. The reluctance torque is measured with opened rotor windings of proposed motor. As shown in Fig. 12, it can be confirmed that the additional torque by E-coils greatly contributes to increase the total output torque. The proposed motor is able to use the electromagnet torque in addition to conventional reluctance torque.

VII. CONCLUSION

This paper has presented a pancake axial-air-gap-type self-excited wound-field synchronous motor where space harmonics power is efficiently utilized for the field magnetization instead of the permanent magnets. The advantage in terms of the torque density has been clarified through the electromagnetic field analysis. In addition, verification of the self-excitation principle generated by the space harmonics power has been demonstrated through the preliminary experimental test results. The future work of this study is to clarify the advantages of the torque density compared with radial-air-gap-type wound-field motor. Furthermore, it will be revealed the motor efficiency of proposed motor and adjustable speed drive characteristics. It is also important to develop the more accurate mathematical model since estimation of the induced current and the field current of the rotor windings is significantly important for the proposed motor.

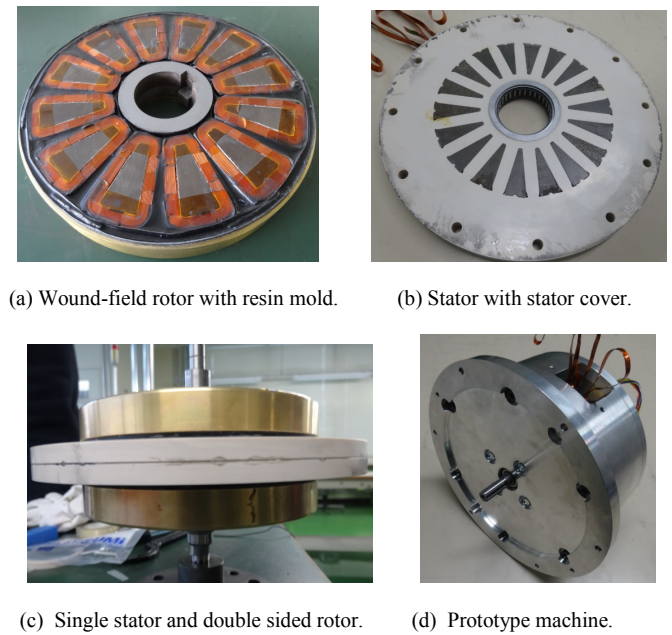


Fig. 10. Prototype machine.

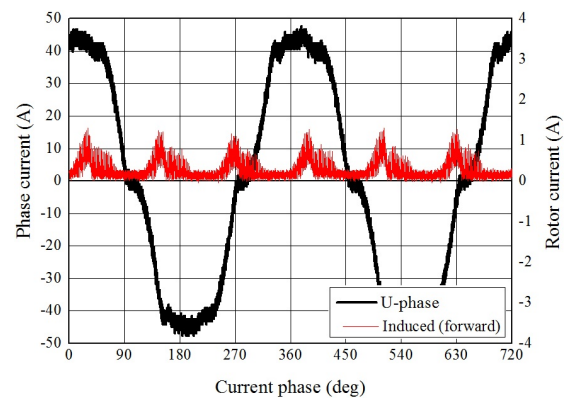


Fig. 11. Stator and rotor current waveform for 500 r/min under 40 A_{rms}.

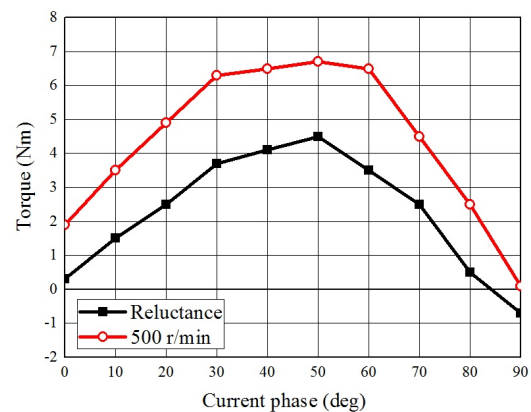


Fig. 12. Current phase vs. torque characteristics under 40 A_{rms}.

REFERENCES

- [1] Y. Sato, S. Ishikawa, T. Okubo, M. Abe and K. Tamai, "Development of High Response Motor and Inverter Ssystem for the Nissan LEAF Electric Vehicle," *SAE Technical Paper* 2011-01-0350, 2011.
- [2] C. Pollock, H. Pollock, R. Barron, J.R. Coles, D. Moule, A. Court and R. Sutton, "Flux Switching Motors for Automotive Applications," *IEEE Trans. I.A.*, vol. 42, No. 5, pp. 1177-1184, 2006.
- [3] T. Kosaka, N. Matsui, Y. Kamada and H. Kajiura, "Experimental Drive Performance Evaluation of High Power Density Wound Field Flux Switching Motor for Automotive Applications," *The 7th IET Int. Conf. on Power Electronics, Machines and Drives (PEMD)*, B8.01-0418, 2014.
- [4] K. Hiramoto, H. Nakai, E. Yamada, N. Minoshima and M. Seguchi, "Rotary Electric Machine and Driving Controller for Rotary Electric Machine," US20100259136 (Published in 2010)
- [5] K. Hiramoto, H. Nakai, "Propoosal and Feasibility Study of the Integrated Diode Synchronous Motor," *IEEJ. Annual Meeting*, No. 5-054, pp. 97-98, 2014. (in Japanese)
- [6] K. Hiramoto, H. Suzuki, H. Nakai, E. Yamada, R. Mizutani, N. Minoshima, "Increment of the Integrated Diode Synchronous Motor in the Low Revolution Speed Area," *IEEJ. Annual Meeting*, No. 5-055, pp. 99-100, 2014. (in Japanese)
- [7] M. Aoyama, T. Noguchi, "Preliminary Study on Rare-Earth Free Motor with Field Pole Excited by Space Harmonics," *IEEJ. Annual Meeting*, No. 5-051, pp. 91-92, 2013. (in Japanese)
- [8] M. Aoyama, T. Noguchi, "Estimation of Rotor Current on Mathematical Model of Wound-Field Synchronous Motor Self-Excited by Space Harmonics," *The 22nd International Symposium on Power Electronics, Electrical Drives, Automation and Motion (Speedam)*, EMD0058, pp.589-594, 2014.
- [9] M. Aoyama, T. Noguchi, "Torque Performance Improvement with Modified Rotor Winding Circuit of Wound-Field Synchronous Motor Self-Excited by Space Harmonics," *IEEJ. Trans. I.A.*, vol. 134, No. 12, pp. 1038-1049 (in Japanese).
- [10] S. Nonaka, K. Kesamaru, "Brushless Self-Excited Single-Phase Synchronous Generator Using Wound Rotor Type Three-Phase Induction Machine," *IEEJ* vol. 101, No.6, pp.743-750, 1981
- [11] S. Nonaka, "The Self-Excited Type Single-Phase Synchronous Motor," *IEEJ. Trans.*, vol. 78, No. 842, pp. 1430-1438, Nov. 1958. (in Japanese)
- [12] S. Nonaka, "The Brushless Self-Excited Type Single-Phase Synchronous Generator," *IEEJ. Trans.*, vol. 82, No. 883, pp. 627-634, Apr. 1962. (in Japanese)
- [13] S. Nonaka and I. Muta, "An Analytical Study of the Brushless Self-Excited Type Single-Phase Synchronous Generator," *IEEJ. Trans.*, vol. 86, No. 934, pp. 1140-1149, Jul. 1966. (in Japanese)
- [14] T. Fukami, Y. Hanada and T. Miyamoto, "Analysis of the Self-Excited Three-Phase Synchronous Generator Utilizing the 2nd-Space Harmonic for Excitation," *IEEJ. Trans. I.A.*, vol. 117, No. 1, pp. 57-65, 1997. (in Japanese)
- [15] M. O. Oliveira, A. S. Bretas, F. H. Garcia, L. A. Walantus, H. E. Munoz, O. E. Perrone and J. H. Reversat, "Design and Analysis of Brushless Self-Excited Three-Phase Synchronous Generator," *International Conference on Renewable Energies and Power Quality (ICREPQ12)*
- [16] S. Li, B. Yuan, "Study on a Novel Brushless Self-Excited and Three-Phase Synchronous Generator with Constant Voltage Output," 2012 International Coferece on Electrical and Computer Engineering (ICECE2012), 978-1-61275-029-3, pp. 47-52 (2012)
- [17] L. F. A. Izzat, S. Heier, "Development in Design of Brushless Self-Excited and Self-Regulated Synchronous Generator," *The 2nd International Conference on Renewable Energy Research and Applications (ICRERA)*, ID374, 2013.
- [18] J. Oyama, S. Toba, T. Higuchi and E. Yamada, "The Principle and Fundamental Characteristics of Half-Wave Rectified Brushless Synchronous Motor," *IEEJ. Trans. I.A.*, vol. 107, No. 10, pp. 1257-1264, 1987. (in Japanese)
- [19] J. Oyama, T. Higuchi, N. Abe, and E. Yamada, "The Principle and Fundamental Characteristics of AC-Excited Brushless Synchronous Motor," *IEEJ. Trans. I.A.*, vol. 109, No. 7, pp. 515-522, 1989. (in Japanese)
- [20] G. Dajaku, D. Gerling t, "New Self-Excited Synchronous Machine with Tooth Concentrated Winding," Document of university of Muenchen.